The generation of 3D flows in a combined current and wave tank

THE GENERATION OF 3D FLOWS IN A COMBINED CURRENT AND WAVE TANK

Adam Robinson*, David Ingram, Ian Bryden, and Tom Bruce.

Institute for Energy Systems, School of Engineering, The University of Edinburgh, Kings Buildings, Mayfield Rd, Edinburgh, EH9 3JL, United Kingdom.

KEYWORDS: **WAVE, CURRENT, TEST, TANK, RANS, CONTROL, GENERATION, SIMULATION, SHEAR, LAYER**

ABSTRACT

One means of producing a 3D current in a circular tank is by using groups of conditioned axial flow impellers arranged around the perimeter to collectively create a sea representative bulk flow in a laboratory setting. Unfortunately to achieve the required bulk flow neighbouring impellers have to operate at different speeds resulting in steps in the plan view velocity profile. Therefore the underlying situation that governs tank behaviour is that of two fluid streams at different speeds combining, leading to a turbulent mixing layer which then dissipates and develops. Here a simulation of this flow is created using a 2D Reynolds Averaged Navier-Stokes method and then validated with physical experiments. The implications for accuracy and computational costs of various turbulence models, boundary conditions setups, and geometry representations are assessed. These findings are then used to produce a simplified 2D numerical model of the plan view flows in a 3D test tank which is then employed to demonstrate how a satisfactory device test zone might be generated from groups of stepped inputs. This finding helps prove that a combined current and wave tank can be created using the described configuration with the model providing a useful means of testing control scenarios.

* Corresponding author: Adam Robinson, Adam.Robinson@ed.ac.uk

1.0 INTRODUCTION

Testing is a necessary part of development for off-shore devices and structures. A current and wave testing tank capable of producing realistic sea conditions at 1:20 scale would provide a mid-step between existing small scale test facilities and sea trials. Figure 1 shows the layout of the first of this new type of test tank which is currently being built at Edinburgh University.

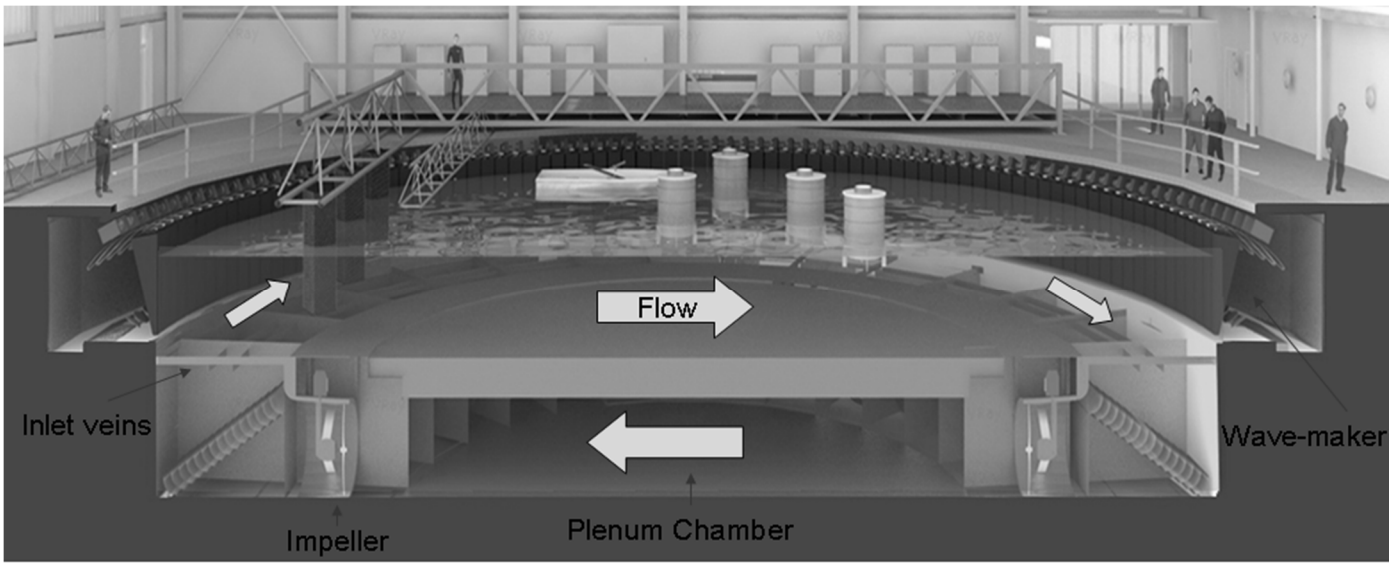

Figure 1 Vertical section through the combined current and wave test facility under construction at the University of Edinburgh.

Figure 2 shows the operational principles, simplified to consist of six separate flow streams. The conditioned flow from the impellers is driven out of guide vanes in the tank floor, and then combined to form a defined flow across the centre of a circular tank, before being drawn back into the plenum chamber. The Edinburgh facility actually uses 28 impellers to achieve this effect. The aim is to create representative sea conditions in a large enough area to test arrays of off-shore devices.

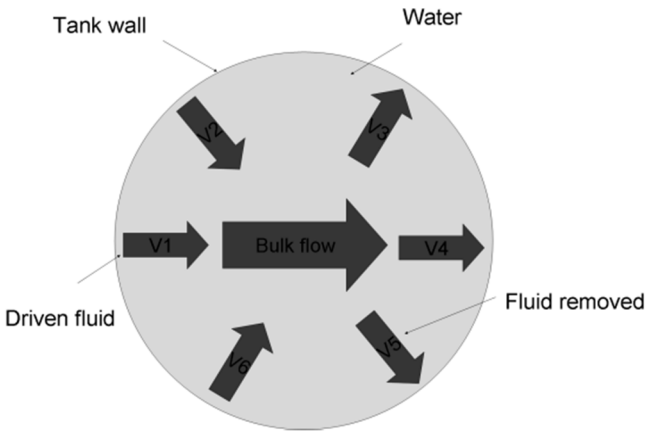

Figure 2 Separate streams of driven fluid combining to form a bulk flow in a tank viewed in a direction aligned with gravity.

Each propeller used to create the bulk flow produces a stream at a single velocity which may be different to its neighbours. This difference in velocity leads to a turbulent shear layer between inlets and can lead to a stepped or curved plan view velocity profile in the test section of the tank where a plug profile is usually required. It is, therefore, necessary to understand and quantify the nature of the shear between individual input streams. This paper will consider the evolution of the shear layers between such inlets. An outline of the simulation is given in Figure 3 where two flows at different velocities combine to create a vertical shear.

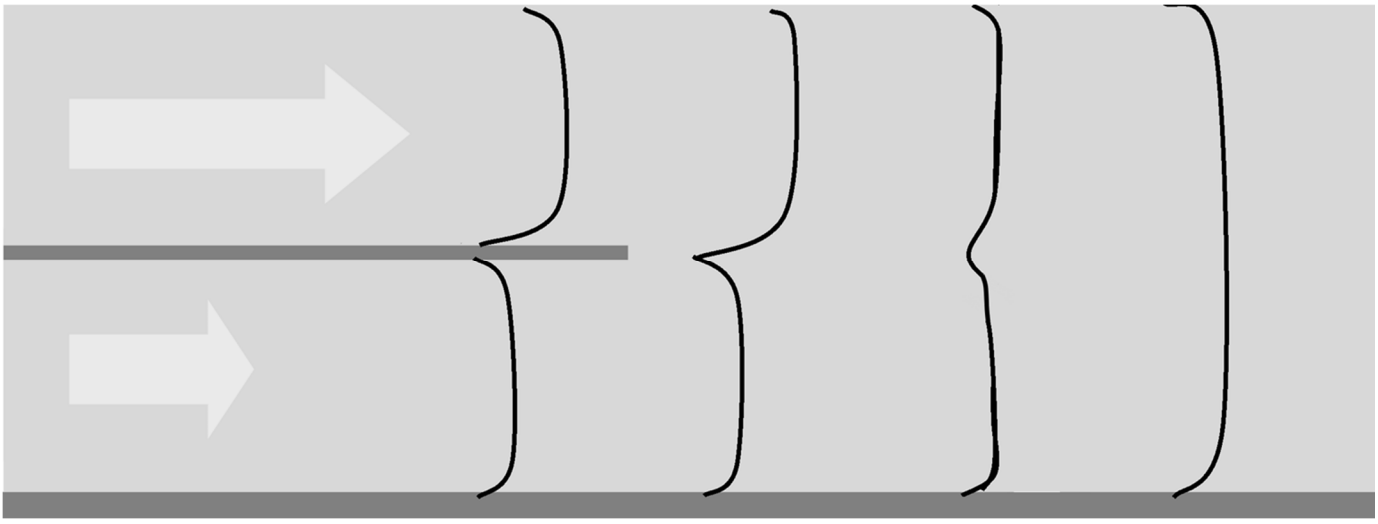

Figure 3 A 2D slice of separate streams of driven fluid combining to form a bulk flow in a flume viewed from the side with gravity aligned down the page. Black lines indicate the type of velocity profile development expected.

The final aim of this study is to support the development of a 3D numerical model of a combined wave and current test facility. It may be necessary to model more than twenty-eight turbulent shear layers each in 3D extending from the free-surface to the tank floor then downstream. Detailed models of the basin will also require waves to be simulated. The choice of numerical model is therefore critical in allowing such simulations to be tractable without recourse to very large high performance computers.

Initially, experimental data from a smaller scale test will be used to validate a Reynolds Averaged Navier-Stokes (RANS) numerical model. This will then be used to predict the development distance and plan view velocity profile in a full scale tank. Along with this, the implication to accuracy and computational cost of various turbulence models approaches to boundary conditions and geometry representation will be explored. The turbulence models tested will include: k -ε standard model; RNG k -ε model; k -ω and Reynolds shear stress approach.

The inlet boundary can be represented in two ways: The first excludes geometry and uses the measured point velocities immediately downstream of the flow combination to provide node values of velocity at the inlet boundary; the second method includes the geometry of the splitter plate between the streams. Excluding the geometry may lead to a reduction in computational cost, without reducing the usefulness of the model to engineering design.

Subsequently, the model will be extended to provide a simplified 2D representation of the 3D tank flows in a combined current and wave tank. Once this extended model is proven to be numerically sound, it will be used to find a combination of inlet settings that generates a plan view velocity profile that is suitable for testing arrays of offshore devices. This generated test area must have a uniform and developed velocity profile and a prescribed level of turbulence to be sea-representative as well as being large enough to allow realistically spacing array of scaled tidal power generation devices.

2.1 NUMERICAL SIMULATION OF TURBULENT MIXING LAYERS

As well as being the dominant factor affecting the behaviour of the 3D flow in a combined current and wave tank, turbulent mixing layers are an important and well-studied phenomenon in fluid dynamics. Turbulent mixing layers are a kind of Kelvin-Helmholtz instability that develops when flows of different speeds combine with significant shear. This results in a 2D span-wise series of vortical structures known as rollers (Loucks and Wallace 2012). Figure 4 is an experimental image showing a turbulent mixing layer.

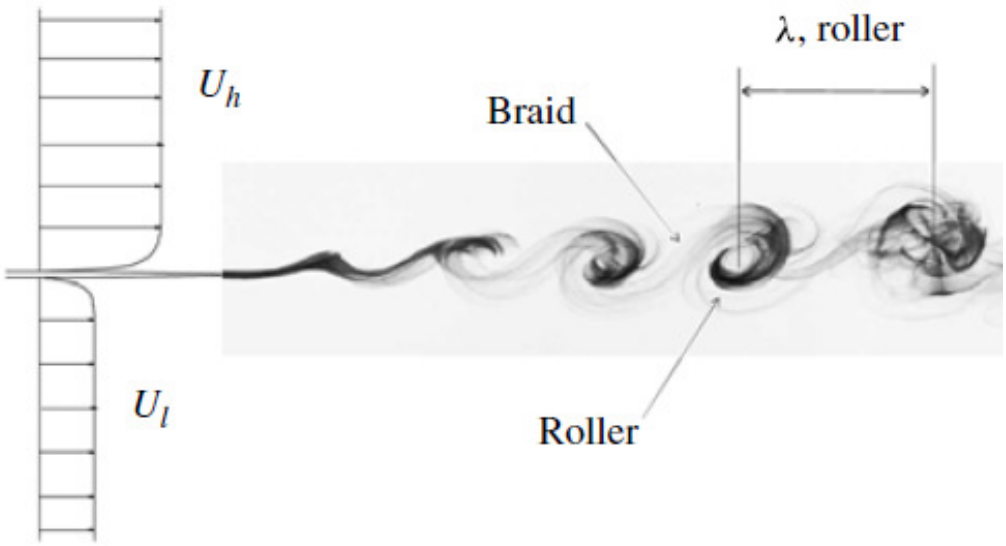

Figure 4 Turbulent mixing layer image (Loucks and Wallace 2012).

A detailed physical explanation of turbulent mixing layers in the context of a combined current and wave tank is given in a previous paper (Robinson, Richon et al. 2014)

Many numerical models have been created to provide a means of predicting and investigating the behaviour of a turbulent mixing layer without having to create a representative experiment. Balaras *et al.* (Balaras, Piomelli et al. 2001) suggests that for turbulent mixing layers, which are very sensitive to small upstream changes, numerical simulations have the benefit of being able to precisely define inputs and the environment when compared to physical experiments.

The typical turbulent mixing layer involves large vortical structures which eventually break down to the Kolmogorov scale, then dissipate due to viscosity. This breakdown is physically complex and therefore requires powerful numerical techniques to produce a representative simulation.

In this work the aim is to accurately simulate how the two separate streams combine after the splitter plate with the turbulent mixing layer eventually developing to form a flow with a uniform single velocity profile. This development may take a length equivalent to a thousand times the diameter of the first roller.

Although simulations of turbulent mixing layers have been attempted analytically by Neu (Neu 1984) and using Lagrangian numerical methods by Ashurst and Meiburg (Ashurst and Meiburg 1988), most attempts have involved numerical solutions of the Navier Stokes equations. The first method in this category is Direct Numerical Simulation (DNS) which attempts to solve the Navier-Stokes equations for all scales of motion.

Rogers and Moser (Rogers and Moser 1992) use DNS in an attempt to answer some questions related to the early development of the mixing layer. Rather than modelling the area the rollers progress through as they move downstream the approach used simulates just the pair of rollers as they develop over time. This method is analogous to moving a picture frame downstream so if always contains the same rollers, reducing the computational requirements. Although this is a useful simplification Comte *et al*. (Ducros, Comte et al. 1996) states that once the upstream perturbations become important a spatially growing simulation is required. The DNS simulation was performed by solving vortices equations derived from the Navier-Stokes equations in a Eulerian grid with a size of 192 x 212 x 128 cells with a method described by Spalart, Moser and Rogers (Spalart, Moser et al. 1991). The simulation is begun in a clean state with one layer moving above the other with no turbulent mixing layer. This is then allowed to run on in time; due to the boundaries being periodic the turbulent mixing layer develops (Moser and Rogers 1993).

DNS is a useful tool when the modelled phenomenon can be resolved on at a single scale accurately resolved with a computable number of grid cells. As the turbulent eddies break down and reduce in size there becomes a point where DNS is impractical. In 2001 Balaras et al (Balaras, Piomelli et al. 2001). stated that DNS using computational grids significantly larger than those done by Rogers and Moser (Rogers and Moser 1994) are prohibitively expensive. Fortunately once the eddies reduce beyond a certain size relative to the bulk flow representing them directly is no longer necessary to achieve a usefully accurate prediction of the bulk flow behaviour. A method that is suited to this kind of phenomena is Large Eddie Simulation (LES) were eddies that are large relative to the bulk flow size are directly simulated using DNS. The effects of the small eddies are represented indirectly by equations known as a sub-grid model. LES uses spatial and sometimes temporal filtered Navier-Stokes equations and choose what features to resolve using a filter function. The simplest sub-grid model that have been shown to be accurate are based on the turbulent viscosity approach to turbulence modelling ie Boussinesq hypothesis, where the effects of turbulence manifest as a modified viscosity.

Comte *et al.* (Comte, Silvestrini et al. 1998) uses LES to simulate a spatially growing turbulent mixing layer. The numerical code used in this study solves the complete Navier-Stokes and LES equations. Sub-grid scale effects are

modelled using a filtered structure function model as described by Ducros *et al*. (Ducros, Comte et al. 1996). Comte *et al.* (Comte, Silvestrini et al. 1998). states that this LES based model can be used at far higher Reynolds numbers than previous DNS simulation. This, along with the ability to compute more complex geometry, makes it a useful design tool for vibration prediction in rocket boosters. The method shown here appears to have the capability to model a series of around five rollers using super-computers current to 1998 although no analysis of capability or the computational power used is given. No sensitivity analysis of grid size or initial conditions is documented by Comte *et al.* (Comte, Silvestrini et al. 1998) the importance of these tests in this context is stated in the later work of Balaras *et al.* (Balaras, Piomelli et al. 2001).

Balaras *et al.* (Balaras, Piomelli et al. 2001) uses LES to further investigate turbulent mixing layers and states that the reduced computational cost allows a large range of parameters to be investigated with greater detail than with DNS. They also note that if the sub-grid model or numerical resolution is poorly selected LES can be very inaccurate. As with Comte *et al.* (Comte, Silvestrini et al. 1998) the complete Navier-Stokes equations are solved for the large scale motions and an eddy viscosity based model is used for the small scales. Sensitivity analysis of grid size, domain size and initial conditions were completed along with positive validation against results obtained by DNS. Therefore Balaras *et al.* (Balaras, Piomelli et al. 2001) states the results can be trusted in terms of mesh resolution and model selection. However the solution was still found to be sensitive to initial conditions and boundary size. Balaras *et al.* (Balaras, Piomelli et al. 2001) concludes with the support of some experimental work that this could be due to real turbulent mixing layers behaviour being highly sensitive. Although this simulation was not spatially growing and uses periodic boundary conditions twenty rollers in three dimensions can be seen within the computational domain showing the development of computational power since the work of Comte *et al.* (Comte, Silvestrini et al. 1998).

An example of a spatially growing 2D simulation of a turbulent mixing layer is given by Bogey, Bailly and Juvé (Bogey, Bailly et al. 2000). Here specific details are given of the computational mesh and computational time and power.

A third method of simulating a turbulent mixing layer could be the use of a RANS model with a turbulence model to provide closure. In this approach there is no attempt to directly model turbulent eddies. Instead it works much like the sub-grid model in LES and describes earlier except it is used for all scales of motion by time averaging the Navier-Stokes equations. In RANS no filtering is applied however grid size determines whether an eddy will be resolved. By

performing a mesh independence study (Oberkampf and Blottner 1997) the effect of resolving eddies on the simulation outcome can be determined.

There is little evidence of this type of model being employed to simulate turbulent mixing layers possibly because the accurate representation of large coherent vortices is critical in the type of study described above.

Previous studies like the ones discussed above have computed as few as two and at most twenty rollers. In this study the area of interest extends far further downstream of the splitter plate and may stretch a distance of a thousand times the diameter of the first roller downstream with the resolution of the rollers less critical than the downstream velocity and turbulence profiles. If a RANS approach accurately predicts the flow of interest here it should therefore indicate that the far field downstream results are insensitive to how well the rollers are modelled before they lose coherence.

The eventual aim of this study is to support the development of a 3D numerical model of a combined wave and current test facility. It may be necessary to model more than twenty eight turbulent shear layers each in 3D extending thousands of roller diameters downstream and thousands of roller diameters deep in one simulation. This situation is many orders of magnitude beyond anything computed to date with DNS and LES where a 3D mixing layer with nineteen rollers downstream and significant depth has only recently been computed by Comte *et al.* (Comte, Silvestrini et al. 1998). With this and the simulation costs given by Bogey, Bailly and Juvé (Bogey, Bailly et al. 2000) a simulation of this magnitude required for a combined wave and current tank may be far in the future using LES or DNS.

The reduction in computational requirements that may result from using a RANS may make tank simulation possible with current computer technology and could provide an accurate prediction that is useful for engineering design and control strategy testing.

Although there are no example of RANS being used for a turbulent mixing layer in the literature there are examples for related flows.

Feng *et al*. (Feng, Olsen et al. 2005) used a RANS based method to investigate turbulent mixing of a confined planar-jet. A confined planar-jet is a jet confined between two jets of lower velocity specifically designed to enhance mixing

(Feng, Olsen et al. 2005). Between the jets a turbulent mixing layer may develop. The visualisation presented does not show eddies with the coherent structure seen in works described earlier although some structure is clear and Feng *et al*. (Feng, Olsen et al. 2005) states that large eddies are present and fully resolved in the RANS simulation

Feng *et al*. (Feng, Olsen et al. 2005) compares downstream mean velocity profile results obtained from experiments with PIV against RANS simulations using the k -ε model (Launder and Spalding 1974). They states that although the comparison is good the development rate of the bulk flow is slightly slower than the experimental result and this is likely due to a lower diffusion rate of turbulent kinetic energy for the RANS model.

The k-ε model contains constants which tune turbulent kinetic energy and its dissipation rate. Feng *et al*. (Feng, Olsen et al. 2005) does not give this information here but it is likely the default values given by Launders and Spalding (Launder and Spalding 1974) were used. These constants were set to give accurate predictions in a wide range of turbulent conditions however they may not be optimum for turbulent mixing layers.

The findings of Feng *et al*. (Feng, Olsen et al. 2005) indicate that a RANS simulation may be successful for turbulent mixing layers although an exploration of the of the k -ε model parameters would have made this more solid.

Liu et al (Liu, Feng et al. 2006). later extends this work using the same experimental setup with an improved PIV approach here eddies are clearly seen in the mixing layer. Liu et al(Liu, Feng et al. 2006). uses again uses a RANS simulations with the k -ε model. The conclusions on the performance of the simulation match those of Feng *et al*.(Feng, Olsen et al. 2005)

Hybrids of spatially filtered LES and the time averaged RANS methods have also been found useful in some situations especially where walls have important effects. Hamba (Hamba 2003) gives a good example of this approach. However it will not be discussed here as wall effects are negligible for the type of turbulent mixing layer of mixing layer investigated in this article.

Based on the gaps in knowledge found in this review into the modelling of turbulent mixing layers the following actions are required to economically enable the accurate simulation of 3D combined current and wave tanks:

- An assessment of RANS performance for mixing layers which takes account for recent turbulence modelling developments.
- An assessment of the importance of simulating the splitter plate geometry on flow development.
- An investigation into the effect of inaccurately prescribing turbulence values on downstream development.

2.2 MODELLING WAVE AND CURRENT TEST TANKS

Although many tanks exist where waves and currents combine none have the capability to combine 3D waves with 3D currents. This work is in support of a new type of tank and therefore will require new solutions. The use of curved and round wave tanks with wave-makers around the perimeter is well developed and is described by Taylor et al. (Taylor, Rea et al. 2003),Naito (Naito 2006) and Minoura et al. (Minoura, Takahashi et al. 2009). The work on 3D currents is limited to one source. Salter (Salter 2001) proposed a design for a tank that combined 3D waves and current and later created a scale model (Salter 2001, Salter 2003, Taylor, Rea et al. 2003). This design generates a 3D current by rotating aerofoils around the parameter of a tank and works on the same principal as a Voith-Schneider Propeller. Salter (Salter 2003) states that testing proved the design generally provides a robust means of producing a 3D current. Although the 3D current method used in the tank described here is different as it uses perimeter inlets like those in the tank proposed by Salter (Salter 2001), supporting the new tank's likely success. The tank proposed by Salter (Salter 2001) does not produce a bulk flow from stepped inlet flows like the tank being investigated here and therefore no further insight can be gained.

Examples of the many numerical combined wave and current tanks created are provided by Buchmann et al. (Buchmann, Skourup et al. 1998) as well as Orloff and Krafft (Ortloff and Krafft 1997). These models were produced to test ocean structures and nether includes waves and current generation as waves and currents are more easily provided by prescribing boundary conditions. Orloff and Krafft (Ortloff and Krafft 1997) describe a RANS based method of producing a combined wave and current tank. The only example of absorbing wave-makers being directly modelled is described by Maguire (Maguire 2011). Maguire (Maguire 2011) uses the flow-3D (Hirt 1988) multi-phase RANS code to simulate the behaviour of a wave-maker both producing and absorbing waves. This work, combined with that of Orloff and Krafft (Ortloff and Krafft 1997), demonstrates that all the capabilities required to directly simulate a 3D combined current and wave tank are feasible within a RANS code.

3.1 NUMERICAL MODEL

A computational model was created to replicate the experiment performed in the related paper (Robinson, Richon et al. 2014).This paper gives details of the experimental setup, with Figure 5 giving only an outline.

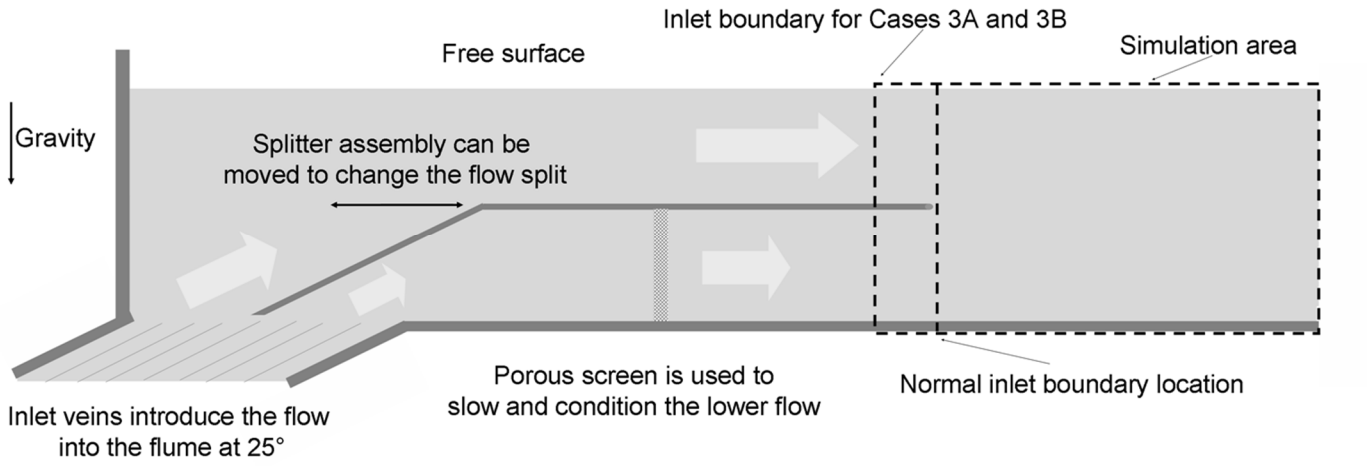

Figure 5 A 2D slice of the experimental setup.

In the experiment a single flow is selectively split in two then separated by a wall; one half is then slowed down and conditioned by a porous screen. It is not necessary to model the entire experiment. The Simulation areas tested are shown in Figure 5.

In the experiment the propeller is set at three different speeds which determine the total flow rate. Three settings for the velocity ratio between the upper and lower stream, giving nine different test conditions in total. Here validation will be carried out using the experimental tests that represent the largest variation in flow conditions.

The computational methodology is based on solving the RANS equations in a Eularian fixed grid implemented within the CFD code FLUENT (Fluent 2006). Various turbulence models are used for closure.

The simulations are run transiently with a variable time step controlled the predictor-corrector type of algorithm proposed by Gresho et al. (Gresho, Lee et al. 1980) and maintaining a truncation error of less than 0.001 until the flow becomes steady. In all cases tested the flow became steady and was to run in a non-time advancing steady mode until the all equation residual reached $1x10^{-7}$.

Second order upwind discretisation is used for the treatment of the advection term except for pressure where the Semi-Implicit Method for Pressure-Linked Equations (SIMPLE) (Issa 1985) algorithm was used.

The flow is simulated in 2D and geometry used for the test is simple, with the boundary conditions providing the complexity of the flow. The geometry is simply a rectangle 0.276m high and 6m long in the flow direction. 6m was found to be long enough that the downstream boundary condition has a negligible effect on the flow in the area of interest.

The upstream inlet boundary condition is set by prescribing node values for u and v velocity, turbulent kinetic energy, *k* and turbulent dissipation rate, *ε* to match that recorded at the corresponding location in the experiment (Robinson, Richon et al. 2014). The velocity is set to the mean experimental value and the turbulent quantities are approximated using Equation 1 and Equation 2 (Fluent 2006). The sensitivity to error of up to 100% in *k* is checked in section 4.3.

$$k = \frac{3}{2}(uI)^2$$

Where:

u = measured velocity

I = measured turbulent intensity

Equation 1

$$\epsilon = c_u^{\frac{3}{4}} k^{\frac{3}{2}} l^{-1}$$

Where:

$C_\mu =$ 0.09

$l =$ Turbulence length scale (0.006m for experiment)

Equation 2

The bottom boundary is set as a wall with a roughness matching the experiment. It was found that modelling the free-surface made little difference to the result and added greatly to the computational cost. The PIV measurements do not extend to the free-surface and would need to be estimated. Due to these factors the upper boundary was set as a free-slip wall.

The physical properties of the water are set within the models based on conditions recorded in the experiments. The values used in the computations were found by using the experimental temperature and the tables provided by White (White 1994):

- Density; water = 996.54 kg/m³
- Viscosity; water = 8.541×10^{-4} kg/m-s
- water temperature 16°C

The mesh created for the computational model is a structured quadrilateral mesh with a higher concentration of cells at the fluid inlet, boundary layers and mixing zone where the separate streams combine.

The basic mesh structure is shown in Figure 6. In the stream-wise direction the mesh expands at a rate of 1.05 from the inlet boundary to the outlet boundary. Across the flow the mesh expands at a rate of 1.05 to the upper boundary from the splitter plate location. Between the splitter plate and the lower wall the mesh expands to the midpoint at 1.1 then contracts again at 1.1 to properly resolve the boundary layer on the bottom wall. This mesh strategy is used throughout.

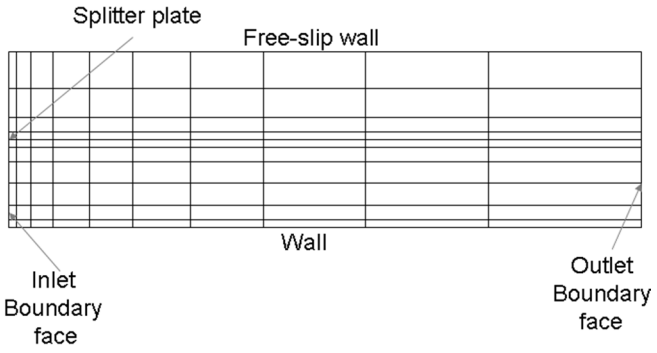

Figure 6 Example mesh

A mesh independence study was completed to ensure that the solutions were independent of the number and location of the cells. This test was computed by creating a series of different meshes with identical geometry and identical boundary conditions. For each mesh the same variable, such as point velocities were recorded. Based on these quantities values a mesh was selected which was shown to offer the same result as one of a higher mesh density.

Mesh independence was checked for every case tested to ensure that error due to mesh resolution was less than 1% throughout.

Due to the fact that the *k*-ε model RNG based method was proven more useful for a low cost mixing layer simulation a more detailed study was conducted to ensure an optimised solution. This investigation is described below.

Using the meshing strategy described above a series of eight simulations was created with total mesh sizes between 227 and 73017 cells.

As the ability to predict the downstream development of the mixing layer is critical, the error in the prediction of the velocity profile 930mm downstream of the splitter plate was chosen as the comparison criteria.

To enable this comparison each of the velocity profile for each total mesh size had to be transposed onto an identical set of Y locations using linear interpolation. The maximum and average deviation from the profile of the mesh with the highest resolution is plotted in Figure 7.

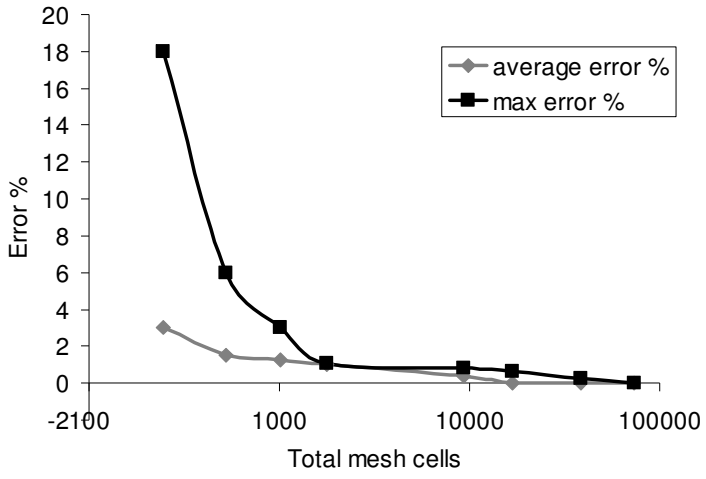

Figure 7 Mesh error vs. the number of cells used for the development of an Identical turbulent mixing layer.

The error remains below 1% when more than 1770 cells are used but if less than this the error greatly increases.

The simulation time for the case with 1770 cells (MI1) is 1620 seconds for 1 second of flow-time with a fixed transient time step of 0.001 seconds.

All equation residuals were converged to 0.0001 and the simulation was carried out on a four core 2.4GHz Intel processor.

3 RESULTS

To investigate the simulation of turbulent mixing layers with RANS and provide the necessary validation for a model of the flow in a combined current and wave tanks a series of tests were carried out. The parameters and results of these are described in Table 1.

Case	u (m/s)	u_h (m/s)	u_l (m/s)	R (m/s)	Initial location x (mm)	Turbulence model	Inlet	Comment
1A	0.62	0.84	0.48	0.57	22.5	*k*-ε RNG	BC	73017 cells
1B	0.62	0.84	0.48	0.57	22.5	*k* -ε STD	BC	
1C	0.62	0.84	0.48	0.57	22.5	R-SST	BC	
1D	0.62	0.84	0.48	0.57	22.5	*k* -ω STD	BC	
1E	0.38	0.5	0.3	0.6	21.7	*k* -ε RNG	BC	
1F	0.59	0.78	0.48	0.62	21.7	*k* -ε RNG	BC	
2A	0.62	0.84	0.48	0.57	22.5	*k* -ε RNG	GEO	Includes geometry
2B	0.62	0.84	0.48	0.57	22.5	R-SST	GEO	Includes geometry
3A	0.62	0.84	0.48	0.57	22.5	*k* -ε RNG	BC	Double turbulence
3B	0.62	0.84	0.48	0.57	22.5	*k* -ε RNG	BC	Half turbulence
MI1	0.62	0.84	0.48	0.57	22.5	*k* -ε RNG	BC	1770 cells

Table 1 Table of cases for single mixing layer simulations.

The investigation will begin with comparison of turbulence model performance against experimental data.

3.1 TURBULENCE MODELS

To achieve an accurate prediction of the mixing layers development the selection of turbulence model is critical. More complete approaches such as Reynolds Stress equation Model (RSM) can give a benefit in accuracy but require more transportation equations to be solved, therefore increasing computational cost. A proven model for mixing layers which add no transportation equations and therefore computationally cheap is the mixing length model (Vesteeg and Malalasekera 2007). However this model is incapable of describing the complex flows and re-circulation that may be present in the full 3D tank model and therefore will not be suitable for the final application. The turbulence models tested here must have the potential to be useful for the final application in combined wave and current tanks. The approaches tested here will be the standard *k* -ε model, the Re-Normalisation Group (RNG) version of the *k* -ε turbulence model, the Wilcox K-ω model and the Reynolds Stress equation Model (RSM).

One of most commonly used turbulence models is the *k* -ε model developed by Launder and Spalding (Launder and Spalding 1974).

This *k* -ε model can account for changes in length and velocity scales and is based on the assumptions (Boussinesq hypothesis) that turbulent behaviour is isotropic and that Reynolds stresses are proportional to the mean rate of deformation.

The *k* -ε model consists of two transportation equations for mean turbulent kinetic energy, k and ε, the turbulent dissipation rate of k.

The equation for k and ε are used here in their standard form proposed by Launder and Spalding (Launder and Spalding 1974), and implemented in the Fluent CFD code (Fluent 2006).

Where this model is used the constants in the standard *k* -ε model are set as:

$C_\mu =$ 0.09 $\quad \sigma_k = 1.00 \quad \sigma_\varepsilon =$ 1.30 $\quad C_{1\varepsilon} =$ 1.44 $\quad C_{2\varepsilon}$ =1.90

The near wall flows are simulated using the standard wall function proposed by Launders and Spalding (Launder and Spalding 1974) where the standard *k*-ε model is used.

A variant of $k-\varepsilon$ tested here is the Re-Normalisation RNG $k-\varepsilon$ turbulence model (Yakhot, Orszag et al. 1992). This model accounts for the effects of small scale turbulence with a random forcing function in the RANS equations. With the RNG model the small scales of motion are removed from the governing equations with their effects expressed in terms of large scale motion and modified viscosity. The RNG versions of the time averaged equation governing k and ε used here were derived by Yakhot et al. (Yakhot, Orszag et al. 1992).

The constants for the RNG *k* -ε turbulence model are set as throughout:

$C_\mu =$ 0.0845 $\sigma_k = 1.39$ $\sigma_\varepsilon =$ 1.39 $C_{1\varepsilon} =$ 1.42 $C_{2\varepsilon}$ =1.68 $\eta_0 =$ 4.377 $\beta =$ 0.012

The result of this is improved predictive accuracy in some rotating flows for little extra computational cost over the standard *k* -ε turbulence model (Yakhot, Orszag et al. 1992) and may be more suitable for the final application. A more detailed description of the model is provided in Vesteeg and Malalasekera (Vesteeg and Malalasekera 2007).

A more complex Reynolds shear stress model, which accounts for turbulent anisotropy and solves an equation for each of the six Reynolds equations, is also tested here. This model was developed by Launder, Reece and Rodi (Launder, Reece et al. 1975). The implementation of the RSM model used in FLUENT is described in the FLUENT user guide (Fluent 2006).

Wilcox *k* -ω model (Wilcox 1988) is also tested for completeness as it has been found to be useful in some general purpose CFD simulations (Vesteeg and Malalasekera 2007).

The cases used to investigate the performance of various turbulence models are detailed in Table 1.

As the ability to predict the downstream development of the mixing layer is critical the error in the prediction of the velocity profile 930mm downstream of the splitter plate was chosen as the comparison criteria.

To enable this comparison the velocity profiles from each case had to be transposed onto an identical set of Y locations using linear interpolation.

The maximum and average deviation from the experimentally measured profile is plotted in Table 2:

Case	Turbulence model	Mean error %	Max Error %
1A	*k* -ε RNG	1.67	3.14
1B	*k* -ε std	1.84	4.18
1C	RSS	2.15	9.2
1D	k-ω	14.3	40
1E	*k* -ε RNG	3.13	10
1F	*k* -ε RNG	4.38	10.6

Table 2 Turbulence model comparison.

The flow in *k* -ω simulation case 1D developed significantly earlier than the experiment leading to large errors. This shows that the default setup of the model is not suitable for mixing layer although a parametric study of the model constants would be need to confirm this. The *k* -ε models gave very similar results at a similar computational cost. The RSS model gave a comparable result to the *k* -ε models but at a computational cost two orders of magnitude higher due to the necessity to solve transiently. A velocity profile comparison of the methods against the experiment is shown in Figure 8. The simulated velocity profiles show a slight difference from the experiment, with all numerical methods showing the same general shape. The velocity profiles provided throughout do not reach the free-surface and only extend to 250mm from the lower wall. This is due to the inability of the experimental technique to measure accurately close to the free-surface (Robinson, Richon et al. 2014). The free-surface would be located 276mm from the lower wall in all figures including Figure 8.

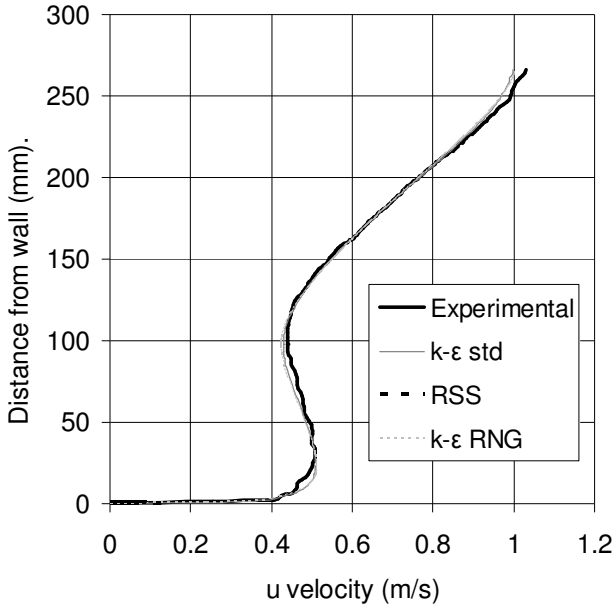

Figure 8 Comparison of velocity profile at x=930mm against experimental data for various turbulence models including; *k*-ε RNG (case 1A), *k*-ε std (case 1B) and RSS (case 1C).

To check that the simulation method was robust two more simulations were set up using the RNG $k-\varepsilon$ turbulence model. The two cases were identical in geometry, model setup and boundary conditions but had different overall velocities and differences shear levels between the mixing layers. The parameters of these tests case 1E and case 1F are given in Table 1.

In general the simulations predict mixing layer development with similar levels of accuracy as with case 1A, Table 2.

Although the general accuracy for case 1E is acceptable, by looking at the velocity profile downstream in Figure 9 it is clear that the prediction is better for the half closer to the free surface than the half close to the lower wall.

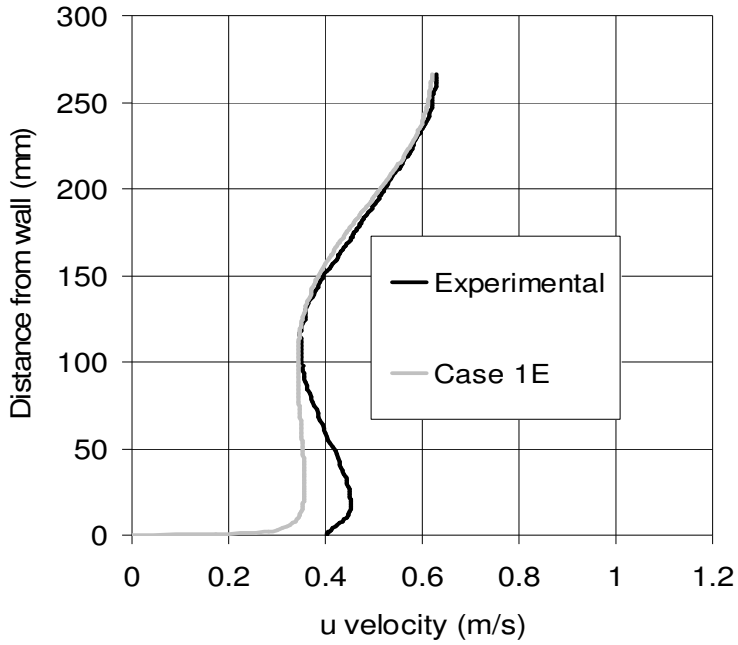

Figure 9 Comparison of velocity profile at x=930mm for Case 1E.

Although the equation constant used in the standard and RNG $k-\varepsilon$ turbulence models were set to best describe a wide range of turbulent situations these settings were found to give acceptable accuracy here. In order to preserve the robustness of the approach for the final more complex application, where other mechanisms may create and dissipate turbulence, it is recommended that the values from the literature are preserved.

3.2 GEOMETRY EFFECT

In the experiment the two streams that lead to the turbulent mixing layer are separated by a splitter plate. The computational domain in the simulations detailed in section 4.1 starts just after the splitter plate removing the need to simulate the splitter plate geometry which reduces computational cost. The implications of this simplification are tested by setting up a simulation that includes the last 100mm of the splitter plate. The computational domain is shown in Figure 5. The *k* -ε RNG model was chosen for this test with all other simulation settings as before.

By analysing the data from each simulation, then comparing the result to the experiment, it was clear that including the geometry had an effect on the downstream wake development. In Figure 10, Figure 11 and Figure 12 It is clear that when the splitter plate geometry is included the prediction of downstream development is slightly improved.

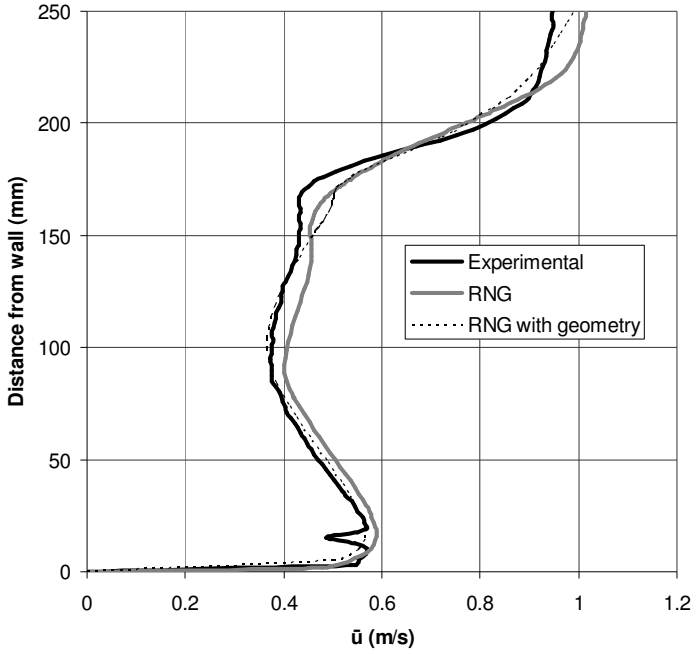

Figure 10 Comparison of velocity profile at x=135mm for Cases 2A (*k* -ε RNG with geometry), 1A (*k* -ε RNG) and experimental data.

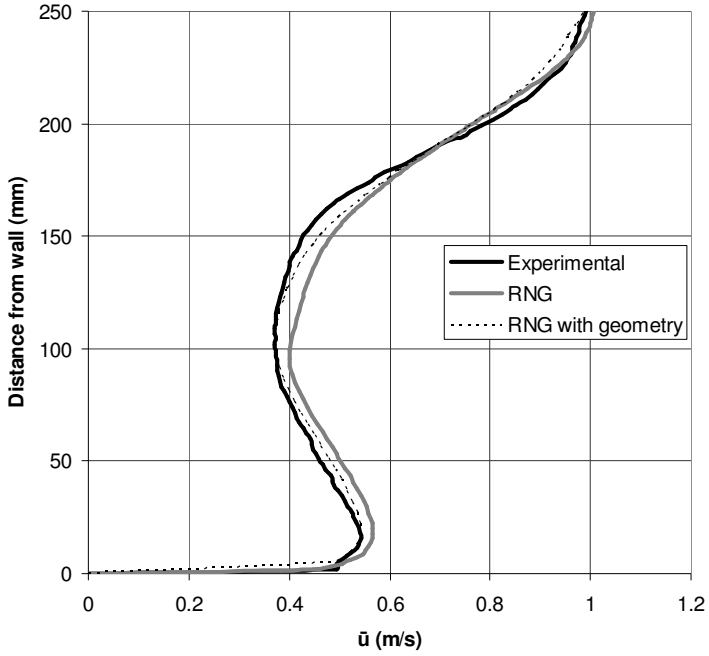

Figure 11 Comparison of velocity profile at x=300mm for Cases 2A (*k*-ε RNG with geometry), 1A (*k*-ε RNG) and experimental data.

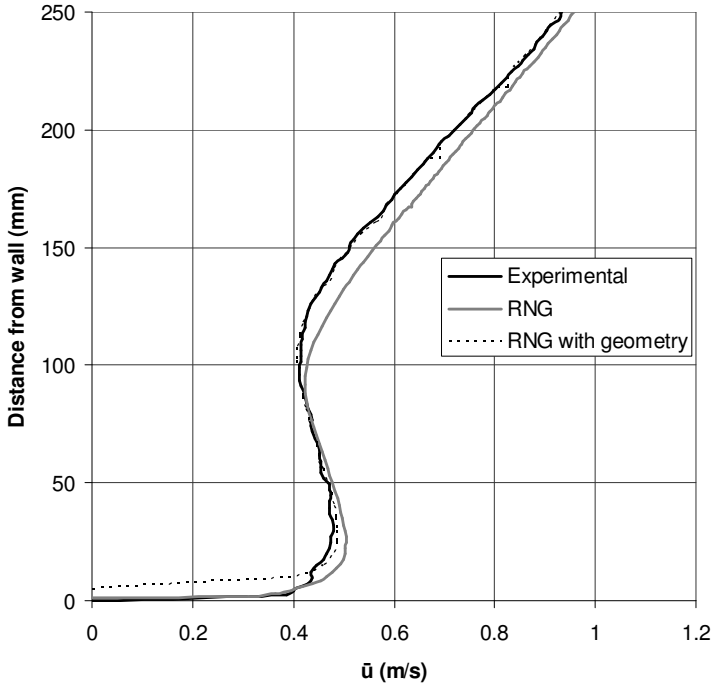

Figure 12 Comparison of velocity profile at x=930mm for Cases 2A (*k* -ε RNG with geometry), 1A (*k* -ε RNG) and experimental data.

The RSS model was also tested with the geometry included and found to have the same effect on development as described for the *k* -ε RNG simulation.

3.3 TURBULENCE ERROR EFFECT

There is some uncertainty in the measurements of turbulence used for the inlet boundary conditions in these simulations due to the experimental method. Here a test is performed to quantify the sensitivity to error in experimental turbulence measurements to the results of CFD recreations of turbulent mixing layers. To investigate these three identical simulations were setup, Table 1. Case 1A uses the experimental turbulence data; Case 3A is the identical but with turbulent kinetic energy doubled. In Case 3B the turbulent kinetic energy is set at half the experimental value. By comparing the downstream velocity profiles at X=930mm for each case the effect of turbulence error can be assessed.

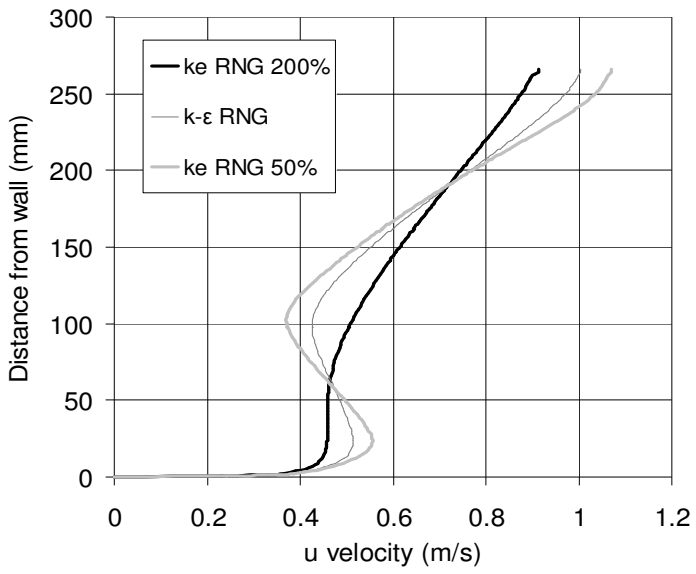

Figure 13 Effects of turbulence error for Case 1A (*k* -ε RNG), Case 3A (*k* -ε RNG 200%) and Case 3B (*k* -ε RNG 50%).

With a 100% error in turbulence the effect on the flow development is significant in terms of the profile shape, Figure 13. The deviation from the velocity profile is around ±4%. This finding shows care should be taken in turbulence

measurements if they are to be used as boundary conditions in a turbulent mixing layer experiment. The measurement technique used to validate and provide the boundary conditions in the simulations presented here had an error of around ±5% for point velocity measurements; therefore the error in profile prediction in this case due to the measurement error should be low.

4.1 3D FLOW IN A COMBINED WAVE AND CURRENT TANK

Having found an efficient and accurate means for predicting the development of a single turbulent mixing layer the method will now be extended to simulate the 3D flows in a simplified combined wave and Current tank. The k-ε RNG turbulence model chosen here was found to be the most accurate and efficient of those tested. Due to the small effect on downstream development the splitter plate geometry is omitted.

To enable the model to be useful for control scenario testing it has to be possible to run many boundary condition setups quickly. With this in mind the tank model was simplified to a 25 metre 2D disc constructed from 28 flat lines. Figure 14 shows how the computational domain and the edges are used as boundary conditions. In the 3D tank configuration shown in Figure 1 the flow is introduced from the bottom of the tank rather than the edges to enable the use of wave-makers. This adds a 3D element that is not accounted for in the 2D model used here. It is not possible to offer at this stage any conclusions about how useful a 2D disc model might be for predicting flows in a tank of this configuration.

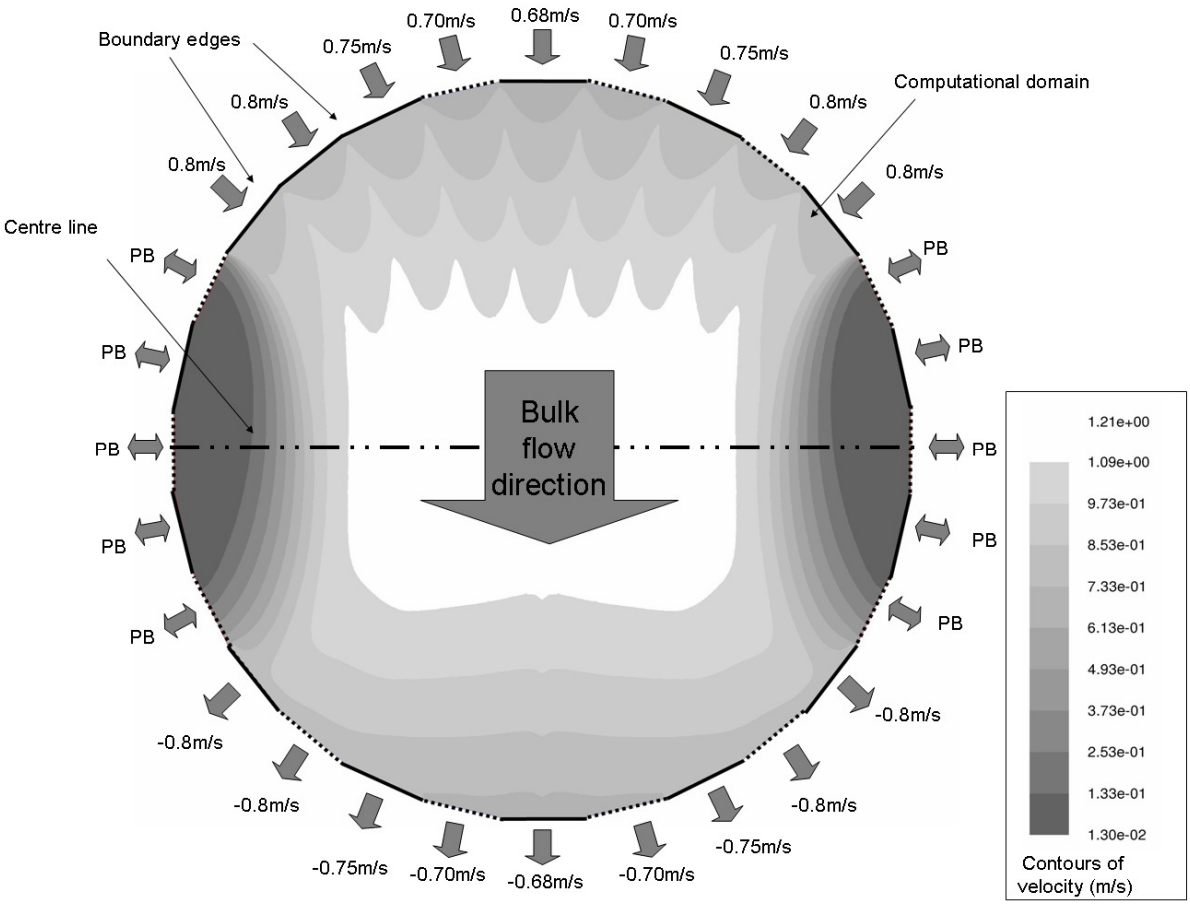

Figure 14 Computational domain superimposed on contours of velocity magnitude plot, the ideal array test area is the white contour at the centre of the tank.

The mesh used to compute this case is based on the structure and density found in section 3.1. A quadrant of the mesh used highlighting two inlet edges is shown in Figure 15.

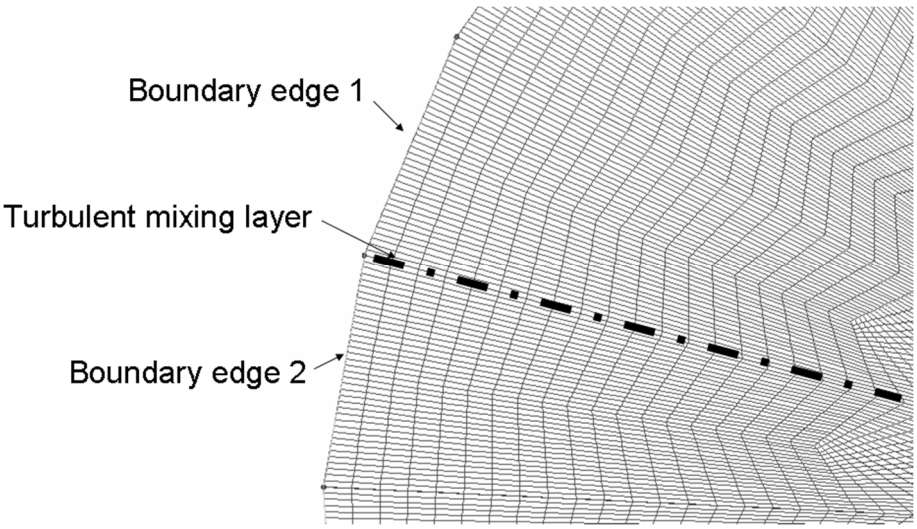

Figure 15 2D disk mesh

To check the mesh strategy was offering the same accuracy demonstrated in Section 3.1 a case was created where the cell count was doubled. This doubled case was then compared to the result of the initial simulation that was created using a mesh resolution based on previous findings. The maximum and average deviation between the centre line velocity profiles (shown in Figure 14) is 0.2% and 0.06% respectively. As before the simulations are run transiently to the same convergence criteria until the flow become steady.

If you had and infinite number of inlets you would have the maximum possible influence over the behaviour in the tank. Unfortunately, due to the 3D nature of the final problem the more inlets you have the smaller the propellers have to be to provide the control input. This increases complexity and reduces efficiency. The compromise between controllability and propeller size chosen here is twenty eight 1.8 metre diameter propellers to drive twenty eight inlets as shown in Figure 14.

The control inputs from the propeller and inlet systems are represented as common boundary conditions. In Figure 14 a boundary condition setup that leads to an acceptable bulk flow pattern is shown. The three condition types used are first a prescribed positive velocity inletting fluid at a fixed rate across the boundary edge; second, a prescribed negative velocity removing fluid at a fixed rate across the boundary edge; and third a Neumann type pressure boundary labelled PB in Figure 14 . The Neumann type pressure boundaries ensure that the net flow in and out of the domain equals zero. This behaviour is analogous to a stationary propeller allowing fluid to pass freely and balances the flows in the way the under-floor plenum chamber would in the real tank, Figure 1. In a physical tank the turbulence level at the inlet is controllable by the design of the inlet vanes and the porous screen that is attached to its underside. Therefore the turbulent intensity can be specified at a uniform 10% with a length scale of 0.005 metres.

To find a suitable boundary condition setup for the twenty-eight inlets an iterative process was used, greatly aided by the ability of the model to produce a converged solution in 60 minutes on the same computer used in section 3.1. The result presented in Figure 14 shows a large usable test area in the centre of the tank (14 x10 metres) where the velocity is relatively uniform and suitable for array testing. The centre line velocity profile (Figure 16) is smooth showing that by this point the turbulent mixing layers are totally dissipated, confirming that this tank configuration is able to provide the necessary performance.

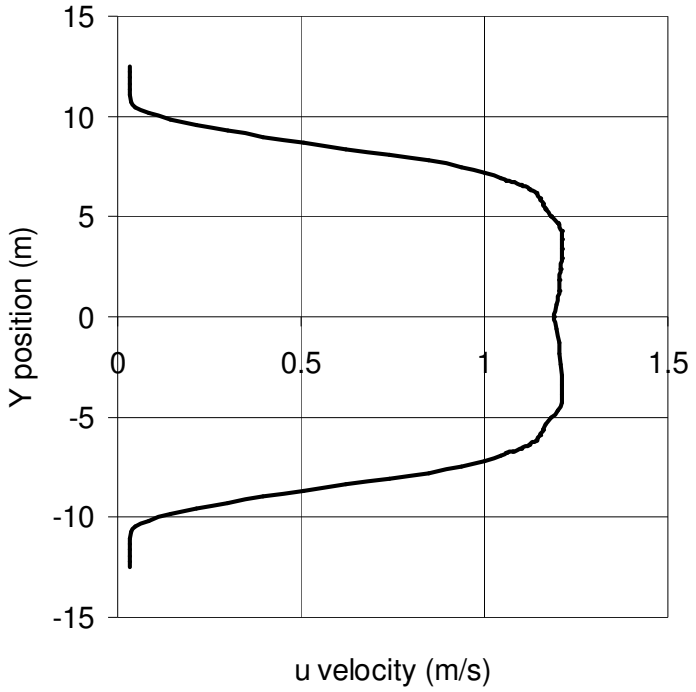

Figure 16 Tank centre line velocity profile.

The results discussed here are strong evidence that a group of conditioned axial flow impeller arranged around the perimeter of a circular tank to collectively create representative sea conditions. The model described can also be used to predict the control inputs to recreate less common sea conditions such as shearing flows and transient behaviour.

4.0 CONCLUSIONS

Although this work has an application to current and wave testing tank design, turbulent mixing layers is a classic fluid dynamic case which can be seen in nature and many engineered flows. Therefore these findings have a wider applicability. The results for the validation case of combining two streams to form a single turbulent shear layer show that the k-ε standard model, RNG k-ε model and a Reynolds shear stress approach all provide accurate predictions of how turbulent mixing layers develop. The RNG k-ε model proved the most accurate with the k-ω model not performing well in its default configuration.

The results prove that RANS is a useful simulation tool for turbulent mixing layers when the far-field development is the critical measure. This also proves that proper resolution of the first rollers and their breakdown is not required to achieve a useful accuracy of far-field downstream development for engineering. This removes the need for DNS or LES and enables the modelling of complex systems containing numerous and sizeable turbulent mixing layers such as combined current and wave testing tanks to be modelled with an available level of computing power.

The inclusion of the splitter plate geometry gives a slight improvement in the accuracy of downstream development prediction however this improvement not significant enough to make the increase in computational time and model complexity worthwhile in the context of a current and wave testing tank.

Having tested the effect of an inaccuracy in the measurement of turbulence it was found that for a given error in turbulence the resulting error in point velocity prediction is twenty-five times less, meaning that PIV results are suitable to provide boundary conditions for simulations.

.

Once the model was validated it was demonstrated that the approach could be extended to a simplified 2D model of the 3D current flows around a combined current and wave testing tank. The model helps prove the concept of using groups of conditioned axial flow impellers arranged around the perimeter of a circular tank to collectively create representative sea conditions over a large enough area to allow the testing of arrays of off-shore devises. The method is also be used to predict the control inputs required to recreate common sea conditions.

ACKNOWLEDGEMENTS

The authors would like to thank the Engineering and Physical Sciences Research Council for funding this research [EP/H012745/1].

REFERENCES

Ashurst, W. T. and E. Meiburg (1988). "Three-dimensional shear layers via vortex dynamics." Journal of Fluid Mechanics **189**: 87-116.
Balaras, E., U. G. O. Piomelli and J. M. Wallace (2001). "Self-similar states in turbulent mixing layers." Journal of Fluid Mechanics **446**: 1-24.
Bogey, C., C. Bailly and D. Juve (2000). "Numerical Simulation of Sound Generated by Vortex Palring in a Mixing Layer." AIAA journal **38**: 2210-2218.
Buchmann, B., J. Skourup and K. Fai Cheung (1998). "Run-up on a structure due to second-order waves and a current in a numerical wave tank." Applied Ocean Research **20**(5): 297-308.
Comte, P., J. H. Silvestrini and P. Guo (1998). "Streamwise vortices in Large-Eddy simulations of mixing layers." European Journal of Mechanics - B/Fluids **17**(4): 615-637.
Ducros, F. R., P. Comte and M. Lesieur (1996). "Large-eddy simulation of transition to turbulence in a boundary layer developing spatially over a flat plate." Journal of Fluid Mechanics **326**: 1-36.
Feng, H., M. G. Olsen, Y. Liu, R. O. Fox and J. C. Hill (2005). "Investigation of turbulent mixing in a confined planar-jet reactor." AIChE Journal **51**(10): 2649-2664.
Fluent (2006). Fluent 6.3 User's Guide. 10 Cavendish Court, Lebanon, NH 03766, U.S.A.
Gresho, P. M., R. L. Lee and R. L. Sani (1980). "On the time-dependent solution of the incompressible Navier-Stokes equations in two and three dimensions." Recent advances in numerical methods in fluids **1**: 27-79.
Hamba, F. (2003). "A Hybrid RANS/LES Simulation of Turbulent Channel Flow." Theoretical and Computational Fluid Dynamics **16**(5): 387-403.
Hirt, C. W. (1988). "Flow-3D Users Manual." Flow Science Inc.
Issa, R. I. (1985). "Solution of implicitly discretised fluid flow equations by operator splitting." Journal of Computational Phys. **62**: 40–65.
Launder, B. E., G. J. Reece and W. Rodi (1975). "Progress in the Development of a Reynolds-Stress Turbulent Closure." Journal of Fluid Mechanics **68**(3): 537-566.
Launder, B. E. and D. B. Spalding (1974). "The Numerical Computation of Turbulent Flows." Computer Methods in Applied Mechanics and Engineering **3**: 269-289.
Liu, Y., H. Feng, M. G. Olsen, R. O. Fox and J. C. Hill (2006). "Turbulent mixing in a confined rectangular wake." Chemical Engineering Science **61**(21): 6946-6962.
Loucks, R. B. and J. M. Wallace (2012). "Velocity and velocity gradient based properties of a turbulent plane mixing layer." Journal of Fluid Mechanics **699**: 280-319.
Maguire, A. E. (2011). Hydrodynamics, control and numerical modelling of absorbing wavemakers. Phd, The University of Edinburgh.
Minoura, M., R. Takahashi, E. Okuyama and S. Naito (2009). Generation of Extreme Wave Composed of Ring Waves in a Circular Basin. Proc 19th Int Offshore and Polar Eng Conf, Osaka, ISOPE.
Moser, R. D. and M. M. Rogers (1993). "The three-dimensional evolution of a plane mixing layer: pairing and transition to turbulence." Journal of Fluid Mechanics **247**: 275-320.
Naito, S. (2006). Wave Generation and Absorption-Theory and Application. Proceedings of the Sixteenth International Offshore and Polar Engineering Conference (ed. JS Chung, M. Kashiwagi, J. Ferrant, N. Mizutani & LK Chien).
Neu, J. C. (1984). "The dynamics of stretched vortices." Journal of Fluid Mechanics **143**: 253-276.
Oberkampf, W. L. and F. G. Blottner (1997). Issues in computational fluid dynamics code verification and validation. Other Information: PBD: Sep 1997**:** Medium: ED; Size: 35 p.
Ortloff, C. R. and M. Krafft (1997). Numerical Test Tank: Simulation of Ocean Engineering Problems by Computational Fluid Dynamics. Offshore Technology Conference.
Robinson, A., J.-B. Richon, I. Bryden, T. Bruce and D. Ingram (2014). "Vertical mixing layer development." European Journal of Mechanics - B/Fluids **43**(0): 76-84.
Rogers, M. M. and R. D. Moser (1992). "The three-dimensional evolution of a plane mixing layer: the Kelvin-Helmholtz rollup." Journal of Fluid Mechanics **243**: 183-226.
Rogers, M. M. and R. D. Moser (1994). "Direct simulation of a self-similar turbulent mixing layer." Physics of Fluids **6**: 903-923.
Salter, S. H. (2001). Proposals for a combined wave and current tank with independent 360° capability. Proceedings Marec 2001, 2-day conference on marine renewable energies, Newcastle, UK, Inst. Marine Eng.
Salter, S. H. (2003). Design and construction of a 360-Degree Flow Table with Control of Velocity Gradient, IGR report to EPSRC GR/R20694/01.
Spalart, P. R., R. D. Moser and M. M. Rogers (1991). "Spectral methods for the Navier-Stokes equations with one infinite and two periodic directions." Journal of Computational Physics **96**(2): 297-324.
Taylor, J. R. M., M. Rea and R. D.J (2003). The Edinburgh curved tank. 5th European Wave Energy Conference, Cork, Ireland.
Vesteeg, H. and W. Malalasekera (2007). An introduction to computational fluid dynamics: The finite volume method, Prentice Hall.
White, F. M. (1994). Fluid mechanics, McGraw-hill.
Wilcox, D. C. (1988). "Reassessment of the scale-determining equation for advanced turbulence models." AIAA Journal **26**(11): 1299-1310.

Yakhot, V., S. A. Orszag, S. Thangam, T. B. Gatski and S. C.G (1992). "Development of turbulence models for shear flows by a double expansion technique." Physics of Fluids **4**(7): 1510-1520.